International Journal of Modern Physics and Applications
Vol. 1, No. 3, 2015, pp. 77-98
http://www.aiscience.org/journal/ijmpa

Modeling of Interfacial Dynamics in Turbulent Two-Phase Flows Using the Level Set Method

Ashraf Balabel*

Mechanical Engineering Dept, Faculty of Engineering, Taif University, Al, Haweiah, Taif, Saudi Arabia

Abstract

In the present paper, the dynamics of turbulent two-phase flow is numerically predicted. The numerical modeling presented here is based on a new developed numerical method called Interfacial Marker-Level Set method, which coupled with the Reynolds averaged Navier-Stokes equations to predict the dynamical behavior of turbulent two-phase flow. The governing equations for time-dependent, axisymmetric and incompressible two-phase flow are described in both phases and solved separately using the control volume approach on structured cell-centered collocated grids. The transition from one phase to another is performed through a consistent balance of kinematic and dynamic conditions on the interface separating the two phases. The topological changes of the interface are predicted by applying the level set approach. The performance of linear and non-linear two-equation turbulence models is also investigated. Generally, the developed numerical method demonstrates a remarkable capability to predict the dynamical characteristics of complex turbulent two-phase flow in many industrial applications.

Keywords

Numerical Methods, Two-Phase Flow, Level Set Method, Capillary Instability, Turbulence Modeling

Received: May 19, 2015 / Accepted: May 31, 2015 / Published online: July 9, 2015

1. Introduction

The complex turbulent two-phase flow can be seen in various industrial and engineering applications such as liquid atomization [[1]], internal engine fuel spraying [[2]] and droplet dispersion in turbulent gas-liquid flow [[3]], inkjet printing [[4]] and flow coating [[5]]. One of the important issues in studying the complex turbulent two-phase flow is the stability and the topological evolution of the moving interface between the two fluids. A great attention should also be directed to the nonlinear behavior in the vicinity of the singular point where the interface separates. According to the high complexity of the physics encountered in turbulent two-phase flow and the intrinsic features of the interface, no accurate and satisfying analytical models can exit to this date. Moreover, the experimental measurements are often difficult to visualize and quantify accurately the interface motion in transitional and turbulent flows.

Recently, the huge evolution of the numerical methods and computer speed has allowed the accurate prediction of many complex turbulent two-phase flows of engineering and industrial relevance. However, the numerical study of such complex flows has been somewhat limited because it poses several great challenges [[6], [7]]. The numerical simulations of the complex turbulent two-phase flow with moving interfaces need both refined turbulence models and accurate numerical methods with higher order numerical discretization schemes. Moreover, in such numerical method, the Reynolds-averaged-Navier-Stokes (RANS) equations are usually coupled to a high accurate and robust tracking method in order to follow the complex topological changes of the interface with accurate prediction of the interface normal and curvature.

Over the last years a large number of computational methods

* Corresponding author
E-mail address: ashrafbalabel@yahoo.com

have been developed for solving turbulent two-phase flows with moving interfaces. However, they all suffer from various limitations. All these numerical methods require the solution of some form of the conservation equations for mass, momentum and energy. The major difficulty is that, the turbulent flow has a much wide range of length and time scales. Therefore, the equations for turbulent flows are usually much more difficult and expensive to solve. Nevertheless, no pretence has been made that any of the previous numerical methods can be applied to all complex turbulent two-phase flows: such as ´universal´ method may not exist.

The main objective of the most previous numerical methods concerning the complex turbulent two-phase flows was to perform reliable and accurate simulations in order to investigate ligament formation, stretching and fragmentation into small scale droplets and to further study the influence of the Reynolds and the Weber numbers on the spray-formation dynamic process [[7], [8]]. However, such computations in the presence of large density and viscosity rations and the singular nature of the interfacial forces provide unique challenges. Moreover, the separation of small droplets is corresponded to a singularity of the equation of motion, which makes the numerical simulations extremely costly, since the region around the singularity requires high resolution. So that it is not surprising that RANS simulation in the nonlinear regimes are few [[6], [9]]. In order to continue through the singularity, some *ad hoc* prescriptions for a continuation have to be invented for each particular case, see [[10]] for more details.

There are many approaches to turbulence modeling of two-phase flows. Previous studies in turbulent complex two-phase flows are carried out in the context of direct numerical simulations (DNS). Some examples of numerical studies of the evolution and structure of turbulent shear layers at free surface can be found in [[11], [12], [13], [14]]. In DNS, the full time-dependent Navier-Stokes and continuity equations are solved numerically. Clearly, the advantages of DNS lie in its independence from any modeling or assumptions. However, for high Reynolds number flow, which is the prevailing circumstances in industrial and engineering applications, DNS could not resolve all physical processes encountered and then DNS is beyond possibility. Moreover, the DNS of the atomization process is challenged by involvement of high complexity of physics, surface instabilities, stretching and breakup of ligaments and droplets producing a multi-scale problem that requires high resolution to undertake. To overcome these computational limitations of DNS, the governing equations of motion are subjected to either Reynolds averaging or spatial filtering, resulting in unclosed terms that require closure relations. The governing equation are then closed, however, the choices of such closure models is not straightforward and has some limitations.

Recently, the increase in computational speed has made large eddy simulation (LES) an attractive approach for modeling of turbulent flows. In such context, the large scale eddies are simulated, while the small scales called the sub-grid scales (SGS) are modeled [[15]]. In industrial level, LES is applied in various cases like, internal flows with complex geometries, flows with large separated area, atmospheric boundary layers, simulation in a combustion chamber, and complex flows with moderate Reynolds number. However, LES is extremely computationally demanding for high Reynolds number flows. Moreover, LES is probably realistic away from a solid boundary, however, it has all the limitations of a simple eddy viscosity models near to a boundary. In general, both DNS and LES are still restricted to simple applications, not to deal with a high-Reynolds number flow.

Nevertheless of the previous comments, LES can be directly applied in free-surface flows, provided that the free surface does not exhibit any significant deformation. However, the presence of the complex topological changes in turbulent two-phase flows has relatively a dynamic interaction with both the resolved and modeled turbulence scales in the flow. This can be referred to the interfacial processes that are not described explicitly in the governing equations. Consequently, the modeling of turbulent flow by LES has consequences in the numerical simulation of turbulent two-phase flows.

Over the past decade, efforts have focused mainly on the construction of two-equation eddy-viscosity models and Reynolds-stress-transport closure. The two-equation k- eddy viscosity model is still representing a good compromise between accuracy and computational efficiency. Therefore, the two-equation eddy viscosity models have been the subject of much research in the last years as they still the most widely used in industrial and engineering applications, even though they fail to predict correctly a number of complex flows. It was calibrated and validated for many kinds of high-Reynolds number turbulent flows [[16], [17]].

The conventional eddy-viscosity models are based on a set of linear Boussinesq stress-strain relations. This approach is attractive from a computational point of view, especially in terms of numerical robustness, and it has a large popularity with CFD practitioners. However, this approach is known to be affected by major weaknesses which can be considered as the source of substantial errors where the gradient of the normal stresses contribute significantly to the momentum balance, or what is called complex strain. Although some of ad-hoc corrections have been made, usually to the length-scale equation, and/or the formulation of alternative

equations for different length-scale parameters, none of these corrections can address the fundamental limitations arising from unrealistic constitutive relations, see for more details [[18]].

The alternative route thus pursued extensively over the past decade has been second-momentum closure which is mathematically complex and numerically challenging and often computationally expensive. Accordingly, it has some limitations in the context of industrial CFD. This has thus motivated efforts to construct models which combine the simplicity of the eddy-viscosity formulations and the superior fundamental strength of second-moment closure. These efforts have given rise to the group of nonlinear eddy-viscosity models.

Nonlinear eddy-viscosity models can be traced back to the work of [[19]]. Such approach is generally found to marginally improve the predicted turbulence intensities. However, relative to the linear models, convergence is mostly difficult to achieve. The most nonlinear eddy-viscosity models utilize constitutive equations which are functions of two turbulence scales (usually k and ε) as well as strain and vorticity invariants, e.g. Craft-Launder-Suga (CLS) model [[20]]. The nonlinear models have been previously applied to a wide range of flows in order to assess the ability of these models to predict anisotropy and streamline curvature effects, e.g. plane and fully-developed curved channel flow [[20]] and turbulent flow around a circular cylinder [[21]]. However, the nonlinear models were not widely applied for turbulent two-phase flows. In such situations, the flow exhibits the combined effects of three-dimensionality and streamlines curvature, interfacial normal stresses and surface instabilities. In relation to the flow of interest here, particular weakness of the linear eddy viscosity models related to turbulence production and insensitivity to streamline curvature can be avoided.

In the present study, the performance of linear and nonlinear k- turbulence models variants is investigated when these models are applied to the complex turbulent two-phase flow simulation. The numerical results obtained are evaluated by detailed comparison with the available analytical and experimental data.

The preservation of the interface shape and the mass conservation properties of individual fluids are of great importance in computations of the turbulent two-phase flows. Recently, a large number of numerical methods have been developed for computing the interface movement and predicting its time-dependent topological changes. The literature review of such methods is quite extensive and comprehensive, therefore only a brief account of some important tracking methods is given.

In general, the available numerical method for computing two-phase flows with moving interface can be categorized as interface tracking and interface capturing methods according to the scheme used for identifying the interface. The interface tracking methods involve essentially explicit computational element or Lagrangian particles moving through an Eulerian grid. Such Lagrangian-based methods can predict the interface location precisely. Also, these methods have the ability to resolve features of the interface that are smaller than the grid spacing of the regular Eulerian mesh [[22]]. However, these methods could not deal with the complex topological changes of the interface such as merging and break-up which require a specified algorithm in order to add or remove marker particles as they get too far apart or too close together [[23]]. Moreover, the geometrical quantities of the interface such normal and curvature are difficult to calculate. These problems are amplified when solving a three-dimensional problem.

The interface capturing methods, in contrast to the interface tracking method, implicitly locate the interface through a definition of a separate phase function that discretized on the fixed Eulerian grid. Among several kinds of interface capturing methods, the volume-of-fluid (VOF) [[24]] and the level set (LS) method [[25]] are the most popular interface capturing methods. Although the VOF method has been widely applied for predicting different complex flows, it suffers from several numerical problems such as interface reconstruction algorithms and the difficult calculation of the interface curvature [[6]]. These numerical problems can, in particular, limit the accuracy and the stability of the numerical method adopted for calculation of two-phase flows, especially when the surface tension is included [[9]]. A comprehensive review for the different VOF methods and their numerical constraints can be found in [[14]].

In contrast to the VOF methods, the level set methods offer highly robust and accurate numerical technique for capturing the complex topological changes of moving interfaces under complex motions. The basic idea of LS method is the use of a continuous, scalar and implicit function defined over the whole computational domain with its zero value is located on the interface. Unlike the VOF method, which divided the spatial domain into cells that contain material function, the LS method divided the domain into grid points that contain the value of the scalar function; therefore, there is an entire family of contours. The interface is then describes as a signed distance function at any time, and consequently, the geometric properties of the highly complicated interfaces are calculated directly from LS function. Moreover, the complex topological changes of interfaces such as merging and breaking-up are handled automatically in a quite natural way without any additional procedure. In addition, the extension

of the LS method to three-dimensional problems is easy and straightforward.

Referring to the previous discussion, the LS methods have seen tremendously in different CFD-applications of diverse areas, e.g. two-phase flows, turbulent atomization, grid generation and premixed turbulent combustion [[26]]. However, the LS methods suffer from numerical diffusion which may cause a smoothing out of sharp edges of interface. The LS function is usually evolved by a simple Eulerian scheme, and consequently, the final implementation of LS methods does not provide full volume conservation, so highly accurate transport schemes are required.

From the numerical point of view, both of the VOF and LS methods has its own advantages and disadvantages. However, the great attention that turned recently on the development of new capturing-LS-based methods has given the superiority to the LS methods in the computations of two-phase flows with moving interfaces. In more recent comparison between LS and VOF methods [[27]], it is concluded that when turbulence is taken into consideration, the VOF technique could capture mean effects; however, difficulties are encountered when computing problems with instabilities or when capturing interfaces with strong deformation, see for more details [[28]]. Therefore, in order to alleviate some of the geometrical problems of VOF method and to improve the mass conservation in the LS method, a large number of coupled LS and VOF methods have been developed, see for more details [[29]]. The resulting approach is completely Eulerian and does not include any characteristics of the front tracking methods.

Recently, another class of hybrid methods has been developed and applied for different two-phase flows applications, e.g. the particle level set method [[30]], the Eulerian level set-vortex sheet method [[31]], the hybrid Lagrangian-Eulerian particle-level set method [[6]], the coupled level set-ghost method [[7]] and the coupled level set-boundary integral method [[32]]. All these methods have been quite successful, however, each method has its own advantages and disadvantages. Consequently, it is difficult to affirm which one is generally superior. The success of each method is dependent on the available computational resources and the description of the problem considered. According to the special features of such hybrid methods, the computational cost is much greater and complex than the classical level set method. Moreover, as a result of the different types of the coupled techniques in hybrid methods, there is usually a time step restrictions to obtain stable schemes. Although the ghost method introduces an attractive way for handling the density and pressure jump of two-phase interface, the discretization of the viscous term is challenging and complex [[7]]. In general, the ghost method results in additional computational cost that becomes very demanding in large three-dimensional simulations.

In the present work, we are concerned with further development of the level set method, which belongs to the group of Eulerian interface-capturing methods. The standard level set formulation is based essentially on the previous work of [[33]] and has become very popular, so that a large amount of bibliography using this method has been published and several types of problems have been undertaken, see for more details [[34]]. In such formulation, the two phases are solved as a single phase with variable properties. The fluid properties are assigned and modified according to the distance to the interface function and by using the smooth Heaviside function [[33]] in order to handle the discontinuity across the interface. The interface is smoothed across a finite thickness region, usually a few grid points thick.

Since the surface tension effects play a significant role in the most important two-phase flow problems such as droplet deformation, bubble motion and liquid ligament breakup, a great attention has been given for the numerical modeling of the surface tension force in two-phase flow simulations. In the context of the standard level set method, the continuum surface force (CSF) model [[35]] has been widely used to model surface tension. In the CSF model, surface tension effect is treated as a body force or as a source term in the momentum equation.

Although the standard level set formulation provides a good solution to the problem of interface advection in two-phase flow, however, it suffers from various numerical problems. The inherent problem resulted from introducing the transition region and the smoothing of the interface discontinuity in a continuum formulation remains challenged [[29]]. This results in smearing of flow properties and variables, forcing them to be continuous across the interface in spite of the appropriate jump conditions. Even if smooth initial data are considered, the interface can lose smoothness and develop singularities in finite time. As a consequence, the numerical simulation using this model cannot be continued past the point of singularity without some sort of artificial regularization being applied [[36]].

The second problem associated with the standard level set formulation is the modeling of the surface tension force by using the CSF method. A striking feature of this method, as reported by [[22]], is the so called spurious currents resulted from the inconsistent modeling of the surface tension force. In some cases, these numerical artifacts may lead to catastrophic instabilities in interface calculations and inaccurate description of steep gradients occurring at the interface. In such cases, the effect of the unbalanced forces acting on the interface can reduce the accuracy of the

calculation. Therefore, it is not surprisingly that till now new surface tension models are continuously developed [[29]].

In the present paper, and in order to alleviate the above numerical problems, new approaches are considered. Firstly, instead of using the continuum formulation of the single phase model [[33]], the momentum equations are solved in the dispersed and the continuous phase separately. The normal and the tangential stresses as well as the kinematic conditions are satisfied on the interface separating the two phases. The splitting of the two phases presents, from our numerical point of view, several advantages over the standard level set approach. The Navier-Stokes equations are solved in both fluids with constant properties. Consequently, the computation of the pressure can be done in a standard way without pressure and velocity oscillations at the interface that are common in two-phase level set methods with large density ratios. Another important advantages, is that the continuity equation is enforced always in both fluids, thus allowing the use of standard collocated methods [[34]].

The second approach presented here is the modeling of the interfacial stresses by introducing a number of interfacial markers at the interface intersections with the computational grid lines. The interfacial stresses are calculated accurately on the markers positions. In contrast to the single phase model in which the interfacial jump conditions are embedded naturally on the governing equation, the jump conditions presented here are treated as a boundary conditions enforced explicitly on the normal and tangential direction of the interface. Therefore, the surface tension model, presented here, ensures that, both the pressure calculated inside the droplet and the surface tension pressures are consistent and dynamically similar, as their effect is determined in the same way. Accordingly, the pressure jump across the interface cancels exactly the surface tension potential at the interface and eliminates the numerical error that might be associated with the inconsistent modeling of the surface tension effects in two-phase flow simulation. The problem of the spurious current is almost diminished, as the pressure gradient that drives the flow field is calculated inside the liquid phase accurately.

The previous approaches have demonstrated a remarkable capability in predicting the dynamics of the interface separating two phases in simple two-phase flow applications in robust and accurate manner [[37]]. Moreover, the accuracy of our models was assessed by comparing the obtained results of oscillating a square droplet under the surface tension effects with those predicted by the CSF model; see for more details [[38]]. However, these models have not been applied in predicting the complex turbulent moving interfaces in a wide range of industrial and engineering applications. Therefore, a challenge test for our models is its implementation in predicting the complex dynamics of the turbulent two-phase flows.

The present work aims at developing a new numerical method, which is capable of capturing the interface dynamics in complex turbulent two-phase flows on the basis of the level set method. An extension of our previous numerical method presented in [[39]] is introduced and a new coupling with linear and nonlinear turbulence models is achieved. The interfacial stresses are modeled by calculating their effects on a number of interfacial markers located on the interface intersections points with the computational grids. Therefore, the presented numerical method is referred to interfacial marker level set method (IMLS). The method is tested on several selected problems for which there are available experimental data, or analytical solution. This work aims also at providing a synthetic and critical work on turbulent two-phase flow simulations in order to develop in the near future an original three-dimensional numerical modeling of incompressible turbulent two-phase flows.

The rest of the paper is organized as follows. In section 2, the RANS equations for unsteady, incompressible turbulent two-phase flows are presented, along with the implemented linear and nonlinear turbulence models. Following, the associated interfacial stresses modeling and the interface capturing LS method are explored. Then, in section 3, the numerical IMLS method applied to solve the complete set of equations is described in brief. In section 4, the developed IMLS is tested numerically and its accuracy is assessed by performing the capillary instability of a cylindrical liquid jet as a validation case. Furthermore, the IMLS is applied for simulating one of the most complex industrial turbulent two-phase flow problem; namely, the impinging of gaseous jet on a liquid interface. Finally, in section 6, conclusions of the present work are drawn.

2. Mathematical Formulations

In the IMLS method, the two immiscible fluids (such as liquid/gas) are treated separately; therefore, two sets of governing equations are introduced. Both fluids are assumed to be governed by the incompressible Reynolds form of the continuity and Navier-Stokes equations with constant properties. In order to extend the governing equations to the existing model of two immiscible fluids, two fluid domains $\Omega_1(t)$ and $\Omega_2(t)$ are considered. Both domains are evolving with time t and satisfying:

$$\Omega = \Omega_1(t) \cup \Omega_2(t), \Omega_1(t) \cap \Omega_2(t) = \varnothing \quad (1)$$

Each fluid has its own material properties ρ_α and μ_α (α=1,2), where the subscript $\alpha = l$ or g indicates the liquid and the gas

phase presented at a given point in space. The discontinuity of the mass density and viscosity arise along the interface Γ denoted by:

$$\Gamma(t):\partial\Omega_1(t)\cap\partial\Omega_2(t) \tag{2}$$

Taking the interaction of the two fluids at the interface into account, the instantaneous local equations of motion (called here RANS equations), in conventionally averaged variables, within each fluid after neglecting body forces can be written in tensor notation for two dimensional, unsteady, incompressible and axisymmetric/plane flows (n=1/n=0), as follows:

$$\begin{aligned}&\frac{\partial}{r^n\partial x_i}\left(r^n\rho U_i\right)=0\\&\frac{\partial}{\partial t}\left(\rho U_i\right)+U_j\frac{\partial}{r^n\partial x_j}\left(r^n\rho U_i\right)\\&=-\frac{\partial P}{\partial x_i}+\frac{\partial}{r^n\partial x_j}r^n\left(\mu\frac{\partial U_i}{\partial x_j}+\rho\Re_{ij}\right)\qquad \text{in}\Omega_\alpha\,(\alpha=1,2)\end{aligned} \tag{3}$$

In the above set of equations, we consider that the upper case denotes ensemble-mean quantities and lower case indicates fluctuating or turbulence quantities; U is velocity vector, ρ is density, μ is viscosity, P is pressure and $\Re_{ij}$ is the apparent turbulent stresses or Reynolds stresses ($\Re_{ij}=-\overline{u_iu_j}$). An overbar is used to denote Reynolds averaging. Different turbulence models have been previously developed in order to model the Reynolds stresses and to close the set of the momentum equations. In the following, the definition of linear and nonlinear k-ε turbulence models is introduced.

2.1. Linear and Nonlinear Turbulence Models

The turbulent characteristics of complex two-phase flows can be obtained by solving the transport equation for kinetic energy k and its dissipation rate ε. In such context, the linear standard two-equation k-ε turbulence model (*STD* k-ε) applied in Ω can be written as follows:

$$\begin{aligned}&\frac{\partial}{\partial t}\left(\rho k\right)+U_j\frac{\partial}{r^n\partial x_j}\left(r^n\rho k\right)\\&=\frac{\partial}{r^n\partial x_j}r^n\left[\left(\mu+\mu_t/\Sigma_k\right)\frac{\partial k}{\partial x_j}\right]+\rho\left(P_k-\varepsilon\right)\end{aligned} \tag{4}$$

$$\begin{aligned}&\frac{\partial}{\partial t}\left(\rho\varepsilon\right)+U_j\frac{\partial}{r^n\partial x_j}\left(r^n\rho\varepsilon\right)\\&=\frac{\partial}{r^n\partial x_j}r^n\left[\left(\mu+\mu_t/\Sigma_\varepsilon\right)\frac{\partial\varepsilon}{\partial x_j}\right]+\rho\frac{\varepsilon}{k}\left(C_{\varepsilon1}P_k-C_{\varepsilon2}\varepsilon\right)\end{aligned} \tag{5}$$

where the turbulent viscosity $\mu_t=C_\mu k^2/\varepsilon$ and $\Sigma_k,\Sigma_\varepsilon,C_{\varepsilon1},C_{\varepsilon2},C_\mu$ are the model constants given as 1, 1.3, 1.44,1.92, 0.09 respectively. The turbulent kinetic energy production rate P_k is given as follows:

$$P_k=\Re_{ij}\frac{\partial U_i}{\partial x_j} \tag{6}$$

The modelling of the production term in the turbulent flow simulation is one of the important tasks as it affected by the approximation of the Reynolds stresses. Models following the Boussinesq assumption (1877) in approximating the Reynolds stresses will be referred to linear turbulence models. In such models, a linear stress-strain relation can be defined as follows:

$$\Re_{ij}=\nu_tS_{ij}-\frac{2}{3}k\delta_{ij} \tag{7}$$

Where ν_t is the eddy viscosity, δ_{ij} is the Kronker delta and S_{ij} is the mean stress tensor defined as:

$$S_{ij}=\left(\frac{\partial U_i}{\partial x_j}+\frac{\partial U_j}{\partial x_i}\right) \tag{8}$$

It is more conveniently to re-express the turbulent stress in terms of the dimensionless anisotropy tensor as follows:

$$a_{ij}=\frac{\overline{u_iu_j}}{k}-\frac{2}{3}\delta_{ij}=-\frac{\nu_t}{k}S_{ij} \tag{9}$$

It is known that the linear eddy-viscosity models could not represent adequately the turbulence physics, particularly in respect of the different rates of production of the different Reynolds stresses and the resulting anisotropy, see for example [[18]]. The nonlinear models mimic the response of turbulence to complex strain by using a nonlinear constitutive relation between turbulent stress and mean rate of strain: i.e. roughly of form:

$$a_{ij}=-\frac{\nu_t}{k}S_{ij}+Q_1\left(S_{ij},\Omega_{ij}\right)+Q_2\left(S_{ij},\Omega_{ij}\right) \tag{10}$$

where the quadratic term Q_1 and the cubic term Q_2 are functions of mean strain S_{ij} and vorticity tensor Ω_{ij} that defined as:

$$\Omega_{ij}=\left(\frac{\partial U_i}{\partial x_j}-\frac{\partial U_j}{\partial x_i}\right) \tag{11}$$

The quadratic eddy viscosity model has showed little width of applicability [[39]]. However, the cubic eddy viscosity

model exhibits advantages over the quadratic model in allowing successful inclusion of normal-stress anisotropy and streamlines curvature effects on turbulence. This model has been proposed in [[40]] and further implemented in [[41]]. In such model, a nonlinear relation for the anisotropy tensor is used:

$$a_{ij} = -\frac{\nu_t}{k} S_{ij} + \frac{\nu_t k}{\varepsilon}\left[C_1\left(S_{ik}S_{kj} - \frac{1}{3} S_{kl}S_{kl}\delta_{ij} \right) + C_2\left(S_{ik}\zeta_{kj} + S_{jk}\zeta_{ki} \right) + C_3\left(\zeta_{ik}\zeta_{jk} - \frac{1}{3}\zeta_{lk}\zeta_{lk}\delta_{ij} \right) \right]$$
$$+ \frac{\nu_t k^2}{\varepsilon^2}\left[C_4\left(S_{ki}\zeta_{lj} + S_{kj}\zeta_{li} \right) S_{kl} + C_6\left(S_{kl}S_{kl}S_{ij} \right) + C_7\left(\zeta_{kl}\zeta_{kl}S_{ij} \right) \right] \tag{12}$$

The model coefficients C_1, C_2, C_3, C_4, C_6, C_7 are given as -0.1, 0.1, 0.26, -10 C_μ^2, -5 C_μ^2, 5 C_μ^2, respectively. The coefficient C_μ is now given by the expression:

$$C_\mu = \min\left[0.09, \frac{1.2}{1 + 3.5\eta + f_{RS}} \right] \tag{13}$$

with

$$f_{RS} = 0.235\left(\max\left(0, \eta - 3.333\right) \right)^2 \sqrt{S_I^2} \tag{14}$$

$$\eta = \left(k/\varepsilon\right) \max\left\{ \sqrt{0.5 S_{ij} S_{ij}}, \sqrt{0.5 \zeta_{ij} \zeta_{ij}} \right\} \tag{15}$$

$$S_I = S_{ij} S_{jk} S_{ki} \Big/ \left(0.5 S_{nl} S_{nl}\right)^{1.5} \tag{16}$$

In the present paper, the nonlinear eddy viscosity model is applied to the complex turbulent two-phase flow in case of the impingement of gaseous jet on a liquid interface for the first time to our knowledge.

2.2. Near-Wall Modeling

The above nonlinear model, as reported by [[42]], should contain additional low-Reynolds-number and near-wall terms in order to account for the wall damping effects. In such context, a very large number of nodes are required in order to resolve the flow right down to the wall. In addition, special viscosity-dependent modifications to the turbulence model are required. Instead of that, the wall effects on turbulence can be evaluated via the wall-function and near-wall-modeling approaches [[43]]. Consequently, the low-Reynolds-number terms in the applied nonlinear model are neglected here.

The wall-function approaches are computationally economical, robust and have been widely used in turbulence simulations. In such approaches, often the buffer layer is neglected and considered in the viscous sub-layer. The incorporated zone lies in the range of $0 < y^+ \le 11.63$. The linear dependence of speed flow from wall distance reads

$$U^+ = y^+ \tag{17}$$

where, $U^+ = \frac{U}{U^*}$, $y^+ = \frac{U^* y}{\nu}$ and $U^* = \sqrt{\tau_w / \rho}$ that called shear or friction velocity.

In the logarithmic layer, (for $y^+ > 11.63$), the Reynolds stresses exceed much viscous effects and the structure of velocity can be expresses in the form of the logarithmic law:

$$U^+ = \frac{1}{\kappa_V} Ln(E y^+) \tag{18}$$

where $E = 9.8$, for smooth walls as assumed in the present work and $\kappa_V = 0.41$ is the Van-Karman's constant. At the wall, the boundary value for the dissipation rate at the first near-wall- point, (identified by the subscript p), can be expressed as:

$$\varepsilon_p = \frac{C_\mu^{0.75} k_p^{1.5}}{\kappa y_p} \tag{19}$$

The near-wall value of the turbulence kinetic energy k_P is computed by solving the complete transport equation for k in the near wall control volume, with the wall shear stress included in the production term and zero normal gradients assumed for k at the wall. The above equations can be used to set the computational boundary conditions within a wall-function approach.

2.3. Level Set Method

In order to describe the complex topological changes of the interface separating the two phases with an elegant, robust and efficient method, the level set approach is applied. Since the original work of the level set method introduced in [[44]], a large amount of bibliography on this subject has been published and several types of problems have been tackled with this method; for instance one can see the cited review [[45]].

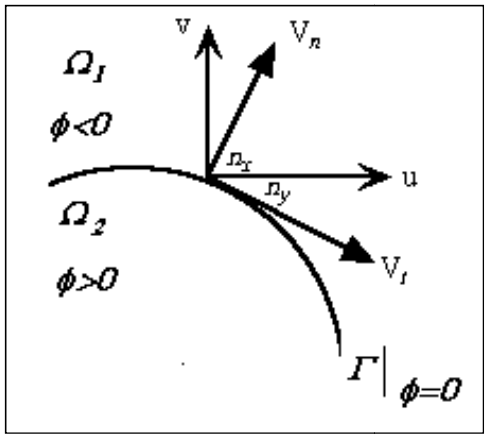

Figure 1. Definition of level set function and velocity components of a moving interface.

The basic idea of the LS method is to embed a moving interface Γ as the zero level set of a smooth phase function ϕ, defined over the whole computational domain. Consequently, the two phases are distinguished by the level set function ϕ(x, t), which can be defined as negative in the dispersed phase and positive in the bulk fluid. Figure 1 shows a moving interface between two immiscible fluids with the definition of the level set function and the projection of 2D velocity components into a normal velocity V_n and tangential velocity V_t according to the normal vectors n_x and n_y in the direction normal and tangential to the interface, respectively.

Mathematically, one can split the velocity components U in the direction of the normal and the tangential of interface in order to get the normal and the tangential velocity; i.e.

$$\begin{pmatrix} V_n \\ V_t \end{pmatrix} = \begin{pmatrix} +n_i & n_j \\ -n_j & n_i \end{pmatrix} \cdot \begin{pmatrix} U_i \\ U_j \end{pmatrix} \tag{20}$$

In the Numerical formulation of the level set, a smooth function ϕ is typically initialized as a signed distance function from the interface i.e. its value at any point is the distance from the nearest point on the interface and its sign is positive on one side and negative on the other. Let us set ϕ as positive in liquid and negative in gas. The location of the interface is then given by the zero level set of the function ϕ. In absence of the interfacial mass transfer such as evaporation or condensation, the equation of the level set method can be written in a form that is equivalent to the Hamilton-Jacobi equation:

$$\frac{\partial \varphi}{\partial t} + V_n |\nabla \varphi| = 0 \tag{21}$$

where V_n is the normal velocity at the interface, defined as V_n = U· n. The unit normal on the interface n, drawn from the liquid into gas, and the curvature of the interface κ can be defined in terms of ϕ as:

$$\mathrm{n} = -\frac{\nabla \varphi}{|\nabla \varphi|}, \ \kappa = \nabla \cdot \mathrm{n} \tag{22}$$

In general, the level set function is advected by using the normal velocity component defined for all the level sets in the computational domain. However, in strictly speaking, the normal velocity has a physical meaning only at the interface location and it is independent of the others away from the interface. Therefore, the thinking about building of extension velocity field in the context of level set methods has received a great attention. One of the most recently developed numerical techniques for constructing of extension velocity filed is proposed in [[46]], where the Fast Marching Method (FMM) proposed by [[47]] is applied. In this method, the normal velocity V_n is replaced by some velocity field F_{ext} known as the extension velocity, which at the zero level set, equals the given speed V_n. In other words;

$$\frac{\partial \varphi}{\partial t} + F_{ext} |\nabla \varphi| = 0 \tag{23}$$

The extension velocity Fext is calculated over the all computational domain Ω by solving the following equation:

$$\nabla F_{ext} \cdot \nabla \varphi = 0, where, F_{ext} = V_n|_{\Gamma} \tag{24}$$

An important step in the solution algorithm of the level set function is to maintain the level set function as a distance function within the two fluids at all times, especially near the interface region, *i.e.* the Eikonal equation, $|\nabla \varphi| = 1$, should be satisfied in the computational domain. By the transient advection of the level set function, it ceases to be the signed distance function, although this property is tacitly employed by applying the FMM [[46]]. However, that is not accurately achieved in case of complex topological changes of the interface. Consequently, in the present work, the re-initialization algorithm described in [[33]] is applied for a specified small number of iterations in the all o computational domain.

The iterative technique developed in [[33]] for re-initializing the level set function is based on solving an additional equation to steady state;

$$\frac{\partial \varphi}{\partial \tau} + \mathrm{sign}(\varphi_o)(|\nabla \varphi| - 1) = 0 \tag{25}$$

where τ is a time-like variable (different from physical time, t), ϕ_o is the initial distribution of the level set function before re-initialization. The sign function $\mathrm{sign}(\varphi_o)$ must be smoothed according to [[33]]:

$$\text{sign}(\varphi_o) = \frac{\varphi_o}{\sqrt{\varphi_o^2 + \beta^2}} \quad (26)$$

Considering regular grid with grid distance h, then, $\beta = h$ and $\tau = h/10$. The above re-initialization technique has proved its effectiveness in preventing inaccurate computations near flat or steep region and preserving as a signed distance function. However, it is somewhat wasteful of computation time due to its iterative nature. Moreover, in some cases, the steady state solution could not be achieved even after a large number of iterations. Therefore, in the present work, a few numbers of iterations is only considered.

2.4. Interfacial Boundary Conditions

Generally, the numerical simulations of two-phase flow could become quite challenging problem and face significant difficulties. In particular, an accurate tracking of complex interfaces, where large deformations and inter-penetration of phases occur, is required. In addition, the basis of improving such numerical simulations lies in satisfying the interface-normal and tangential stress boundary conditions more accurately.

The accurate boundary conditions at the interface separating two immiscible fluids are the balance of the dynamic stresses and the kinematic conditions. Assuming the stress tensor for turbulent flow of an incompressible fluid is given by:

$$\Im_{ij} = -p\delta_{ij} + \mu S_{ij} + \rho\Re_{ij} \quad (27)$$

This equation is applied at each point in the flow field; however, this equation loses its generality at the interface between the two phases as a result of the discontinuous fluid properties. The surface tension effect is known to balance the jump of the normal stress along the fluid interface [[35]]. In case of two immiscible fluids, the interfacial boundary conditions or jump conditions can be written as:

$$[\Im_{ij}].\mathrm{n} = -(\sigma\kappa\mathrm{n} + \nabla_t\sigma) \quad (28)$$

where σ is the surface tension coefficient and the bracket denotes the jump of the stresses along the fluid interface Γ. The unit normal vector n is taken from liquid phase to gas phase and t is an arbitrary vector perpendicular to the normal to the interface. The second term on the right hand side of the above equation is the stress due to gradients on surface tension or Marangoni effect [[48]], usually important when a temperature gradient is applied parallel to the interface, e. g. thermo-capillary convection.

Taking the projections of the jump conditions in the directions normal and tangential to the interface, considering a constant surface tension, one obtains the following two equations in the normal and tangential directions, respectively:

$$[p - \left(\left(2\mu \mathrm{U}_{i,j} + \rho\Re_{ij}\right)\cdot \mathrm{n}\right)\cdot \mathrm{n} = \sigma\kappa\mathrm{n} \quad (29)$$

$$[\left(\left(\mu \mathrm{U}_{i,j} + \rho\Re_{ij}\right)\cdot \mathrm{n}\right)\cdot \mathrm{t} + \left(\left(\mu \mathrm{U}_{i,j} + \rho\Re_{ij}\right)\cdot \mathrm{t}\right)\cdot \mathrm{n}] = 0 \quad (30)$$

It is clear that, according to the approximation of the Reynolds stresses (i.e. linear or nonlinear turbulence model is used), the normal and the tangential boundary conditions could be estimated.

Starting from the Continuum Force Model (CFM) [[35]], the standard level set formulation for incompressible and viscous two-phase flows is based on expressing the surface tension effect in term of a singular source function defined in the momentum equations [[49]]. Consequently, the interfacial jump condition at the interface is integrated into the Navier-Stokes equations, resulting in a body force concentrated on the interface. By using this formulation, a large amount of bibliography has been published and several types of problems have been tackled; see for instance the cited review [[34]].

Although the standard level set formulation provides a good solution to the problem of interface advection, however, the accurate representation of the surface tension force remains a problem when using fixed grids. A striking feature of this method, as reported by [[50]], is the so called "spurious" currents. These numerical artifacts result from inconsistent modeling of the surface tension force and the associated pressure jump. In some cases they may lead to catastrophic instabilities in interface calculations. More generally, these numerical artifacts introduce the problem of obtaining an accurate representation of the steep gradients occurring at the interface. In such cases, the effect of the unbalanced forces acting on the interface can reduce the accuracy of the calculation. Therefore, it is not surprisingly that till now new surface tension models are continuously developed [[51]].

Moreover, the CFM considers that the effect of surface tension is to balance the jump of the normal stress along the fluid interface between two inviscid fluids having a constant surface tension coefficient. Consequently, the interfacial jump condition is reduced to Laplace's formula for the surface pressure [[52]] due to the dropping of the viscous stresses. The effect of neglecting the interfacial shear stress can be seen through increasing of the normal stress magnitude at the phase boundary [[53], [54]]. Moreover, the formation of the capillary ripples on a thin liquid film is dependent on receiving their energy essentially from the pressure and shear stress exerted at the interface by the flowing concurrently high velocity gas stream [[55]].

In contrast to the previous two-phase numerical methods, in which the interfacial jump conditions are embedded naturally on the formulation, the jump conditions at the interface between the two immiscible fluids are treated here as boundary conditions for pressure enforced explicitly at the interface. This numerical technique has bee implemented in our previous work [[38], [39]], and good results have been obtained for a number of challenging problems.

The idea of our modeling is straightforward. By introducing a number of so called "Interfacial Markers" on the intersection points of computational grids with the interface, the surface tension force (mainly the surface pressure) is evaluated and then it is used to drive the liquid phase through the pressure gradient seen in the momentum equations. Moreover, at the position of the interfacial markers, the local curvature is easily estimated by means of a simple interpolation technique. Once the curvature is known, the surface tension force is evaluated. In addition to that, the calculation of the differential terms in the momentum equation can be calculated by means of the appropriate values of the properties at the interfacial marker and by using the actual distance to the interface.

The present surface tension model ensures that both the pressure calculated within the liquid phase and the surface tension pressure is consistent and dynamically similar, as their effect is determined in the same way. Accordingly, the pressure drop across the interface cancels exactly the surface tension potential at the interface.

For more generality of the present model, see figure 2, it is considered that the interfacial pressure inside the liquid phase p_l is determined by evaluating the interfacial pressure in the gas phase p_g and other different "pseudo pressure" terms. i.e.

$$p_l = p_g + p_\sigma + p_\mu + p_{gr} \tag{31}$$

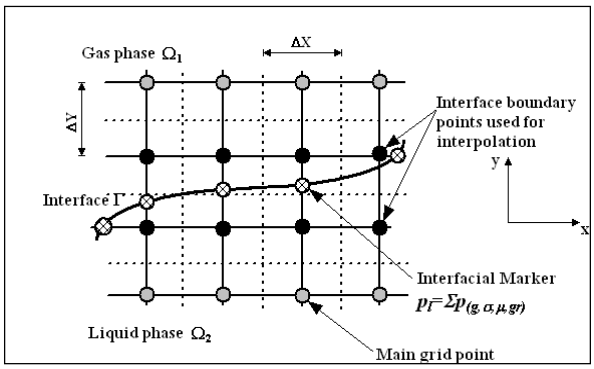

Figure 2. Computational grid point definition.

where p_σ, p_μ and p_{gr} give the interfacial "pseudo pressure" associated to the surface tension effect, the viscous normal stresses and the buoyancy effect, respectively. In such context, the present model enables us to simply include any external interfacial driving force in the pressure boundary condition instead of incorporating it as a body force in the momentum equations. The pressure values calculated from the above equation is then used as Dirichlet boundary conditions for solving the Poisson equation for the pressure. Consequently, this model can in principle be applied to any immiscible fluids problem as long as the stress on the second phase can be specified or neglected.

In the tangential direction, an equality of the shear stress on both sides of the interface should be satisfied; i.e.

$$\mu\frac{\partial V_t}{\partial \mathrm{n}} + \rho\Re_{ij}\Big)_l = \mu\frac{\partial V_t}{\partial \mathrm{n}} + \rho\Re_{ij}\Big)_g \tag{32}$$

In addition to the equality of the dynamically interfacial stresses described above, the kinematic conditions should also be considered. When there is no mass transfer through the interface, the kinematic conditions is satisfied at the interface by assuming the continuity of the normal velocity component, i.e.

$$V_n\big|_l = V_n\big|_g \tag{33}$$

The satisfying of the previous interfacial boundary conditions is an important task in the numerical simulation of two-phase flows as the pressure and velocity field inside the liquid phase are caused by the external gas field normal and tangential stresses. Therefore, the exact pressure level inside the liquid phase, which considers as the driving force, must be specified. The above interfacial conditions are reduced to Laplace's formula [[35]] for the surface pressure in case of inviscid incompressible fluids with constant surface tension coefficient.

In order to obtain the dynamic balance between two immiscible fluids, the complete set of the governing equations are solved for the gaseous field to obtain the velocity, pressure, viscous stresses and any existing force around the interface. These are used as boundary conditions for the solution of the Poisson equation for pressure inside the liquid phase. Further, the governing equations in the liquid phase are solved. Consequently, after getting the complete flow field dynamics, the advection of the liquid interface is carried out using the level set approach.

3. IMLS Numerical Scheme

Recently, different computational fluid dynamics numerical methods for two-phase flows have been developed. These numerical methods can be distinguished by their ways of determining the pressure filed or their techniques to capture

the interface separating the two immiscible fluids. In general, the calculation of the accurate pressure field has the most important effect on the topological changes of the interface rather than other fluid variables.

The standard level set method for incompressible two-phase flows, originated nearly twenty years ago [[33]], has become very popular. In this method, the instantaneous local momentum equations within each fluid are solved with appropriate numerical scheme. However, the direct solution of the momentum equations in such case is naturally difficult, since the fluid properties change discontinuously across the interface, and the concentrated surface tension also becomes infinite in an infinitesimal volume. To overcome these difficulties, the interface is smoothed a cross a finite thickness region, usually a few grid points thick. Moreover, the fluid properties are smoothed according to the Heaviside function that depends on a parameter describing the thickness of the interface or in other words a "transition region", see for more details [[56]].

The most important drawback encountered in the standard level set method is the introduction of the transition region which results in smearing of flow properties and variables, forcing them to be continuous across the interface in spite of the appropriate jump conditions. Even if smooth initial data are considered, the interface can lose smoothness and develop singularities in finite time. As a consequence, the numerical simulation using this method cannot be continued past the point of singularity without some sort of artificial regularization being applied [[57]]. The other drawbacks such as the surface tension modeling and the spurious current problem have been discussed previously. Although the problem of the transition region is solved on the Ghost Fluid Method [[58]], the resulting approach introduces an additional computational cost that can be very demanding in 3D numerical simulation.

In contrast to the standard level set method, in the present paper, the two phases are solved separately using the control volume approach on structured cell-centered collocated grids. The splitting of the two phases presents, from our point of view, several advantages over the standard level set approach. The Navier-Stokes equations are solved in both fluids with constant properties. Consequently, the computation of the pressure can be done in a standard way without pressure and velocity oscillations at the interface that are common in two-phase level set methods with large density ratios. Another important advantages, is that the continuity equation is enforced always in both fluids, thus allowing the use of standard collocated methods without usual pressure and velocity oscillations that occurs at the interface separating the two phases, see for more details [[34]]. The interface is captured with appropriate enforcement of the jump conditions and still retaining the advantages of the level set method. The problem of the spurious current can be decreased, as the pressure gradient that drives the flow field is calculated inside the liquid phase accurately.

More recently, the author has developed a numerical method to track the interface separating two immiscible fluids and to follow its complex topological changes [[38], [39]]. In the present work, we extend our numerical method to turbulent two-phase flows simulation with moving interface. The turbulent characteristics are predicted either by linear or nonlinear turbulence model. In brief, this numerical method is described in the following.

The governing equations are discretized and solved using the implicit fractional step-non iterative method on the basis of the control volume approach proposed by [[59]]. As a result of the complexities introduced by the staggered grid system in two-phase flow calculations and the need to track the liquid surface, a non-staggered grid system is applied here, which requires the use of a single cell network for all variables and a collocated specification of variables at the centre of each cell. High-order approximation for calculating the fluxes at cell faces is applied to prevent pressure oscillations [[39]]. As there is no pressure transport equation necessitates the consideration of the continuity equation, the Poisson equation for pressure is solved by means of the Successive Over-Relaxation method.

In our algorithm, the implicit fractional step-non iterative method is applied to obtain the velocity and pressure filed by presuming that the velocity field reaches its final value in two stages; that means

$$\mathbf{U}^{n+1} = \mathbf{U}^{*} + \mathbf{U}_{c} \tag{34}$$

where by, $\mathbf{U}^{*}$ is an imperfect velocity field based on a guessed pressure field, and $\mathbf{U}_{c}$ is the corresponding velocity correction. Firstly, the 'starred' velocity will result from the solution of the momentum equations. The second stage is the solution of Poisson equation for the pressure:

$$\nabla^{2} p_{c} = \frac{\rho}{\Delta t} \nabla \cdot \mathbf{U}^{*} \tag{35}$$

where Δt is the prescribed time step and p_{c} is called the pressure correction. Once this equation is solved, one gets the appropriate pressure correction, and consequently, the velocity correction is obtained according to:

$$\mathbf{U}_{c} = -\frac{\Delta t}{\rho} \nabla p_{c} \tag{36}$$

This fractional step method described above ensures the proper velocity-pressure coupling for incompressible flow

field. However, the accurate solution of the surface pressure occurring at transient fluid interfaces of arbitrary and time dependent topology enables an accurate modeling of two- and three dimensional fluid flows driven by surface forces. Assuming that a square regular mesh is used for the calculation, the curved shape of the interface causes unequal spacing between the interface and some internal grid points, as illustrated in figure 3. In the present work, a linear interpolation is used to assign values of any variable ϕ at the interface from the known internal grid points values. In addition to that, a finite difference approximation to the derivatives at interface neighboring points is developed.

Referring to figure 3, the interphase boundary value for any arbitrary variable ϕ can be calculated according to the following relation:

$$\phi_B = \phi_A + f\left(\phi_P - \phi_A\right), f = \frac{h_a + h_b}{h_a} \tag{37}$$

Consequently, an approximation of the Laplace equation for pressure at point p is made as follows:

$$\nabla^2 p \approx \frac{2}{h_b + h_a}\left(\frac{p_B - p_p}{h_b} - \frac{p_p - p_A}{h_a}\right) + \frac{2}{h_d + h_c}\left(\frac{p_D - p_p}{h_d} - \frac{p_p - p_C}{h_c}\right) \tag{38}$$

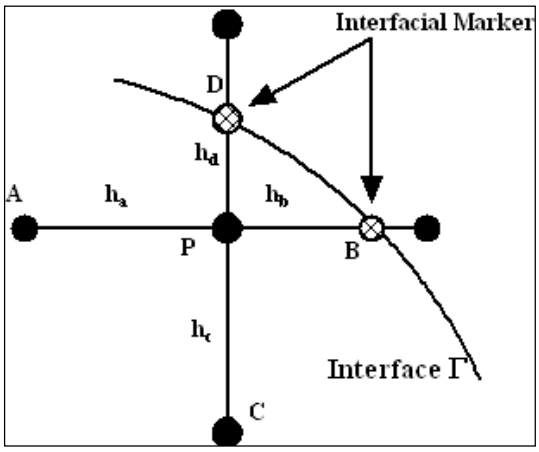

Figure 3. Irregular mesh caused by the interface.

The above equation can be developed utilizing Taylor-series expansion about the grid point p. It can easily be shown that the above formula is equivalent to the regular grid formula if the distances $h_a = h_b = x$, and $h_c = h_d = y$. More details about the numerical procedure used to solve the above system of equations can be found in [[37]].

The above algorithm is applied in a separate way in both phases to obtain the fluid variables in each phase. By using the velocity and pressure values on the gas phase as a boundary conditions defined on the interface, the solution of the liquid phase is carried out. After the whole computational domain is calculated, the turbulent equations are solved on both phases simultaneously. The normal velocity at the interface is then used to move the interface using the level set approach and to obtain its topological changes. Consequently, the whole algorithm is repeated until it would reach the statistically steady state condition.

4 Results and Discussion

In this section, the validation of our developed IMLS numerical method is carried out through performing of two challenge problems of two-phase with moving interface in laminar and turbulent flows. The first case is dealt with the capillary-driven instability of a cylindrical liquid jet in inviscid and viscous regimes. The interfacial boundary conditions in such case are dependent on the surface tension force and the viscous stresses. The effect of the viscous force on the break-up process of the liquid jet in the final stages of evolution is clarified. The second performed problem is the deformation of liquid interface upon the impinging of turbulent gaseous jet. In such case, the interfacial boundary conditions are affected by the surface tension force, the viscous stresses, the gravity force and the turbulence quantities. A new dimensionless number, called Impinging number (IM), which describe the impinging process and the related operating parameters is introduced. For both cases, only a sample of the obtained results is presented, where detailed analysis of both cases will be done in separate and future work. The presented numerical results for the two cases are compared with the linear analysis and the available experimental measurements.

4.1. Capillary-Driven Free Surface Flows

The capillary-driven free surface flows can be found in various industrial applications, e.g. inkjet printing, fuel spraying and atomization of liquid jet. The challenge problems associated with the numerical simulation of such cases are the appropriate modeling of the interfacial stresses (e.g. surface tension and viscous forces) and the choice of the tracking method. An extensive review of such problems can be found in [[29]]. Therefore, in the present work, the numerical simulation of the capillary-driven free surface flows is performed in order to evaluate the capability of the proposed numerical method to capture the interfacial stresses-driven instabilities.

By considering an axisymmetric disturbance is imposed on a cylindrical liquid jet surface, the initial wave profile is assumed to be:

$$r = r_0 + \eta_0 \cos(\frac{2\pi}{\lambda} x) \tag{39}$$

where r_0 is the undisturbed radius of the jet, η_0 is the initial disturbance amplitude and λ is the wavelength of the disturbance. Following the general linear theory provided by Sterling and Sleicher [[60]] for the prediction of the growth rate of the initial disturbance of an inviscid as well as viscous liquid jet and assuming that the liquid jet is driven only by capillary instability and neglecting the effect of the ambient gas, one can obtain the following equation for the growth rate :

$$\omega^2\left[\frac{\xi}{2}\frac{I_0(\xi)}{I_1(\xi)}+\frac{\rho_g\xi}{2\rho_l}\frac{K_o(\xi)}{K_1(\xi)}\right] +\omega\left[\frac{\mu_l\xi^2}{\rho_l r_0^2}\left(2\xi\frac{I_0(\xi)}{I_1(\xi)}-1+\frac{2\xi^2}{\xi_1^2-\xi^2}\left(\xi\frac{I_0(\xi)}{I_1(\xi)}-\xi_1\frac{I_0(\xi_1)}{I_1(\xi_1)}\right)\right)\right] = \frac{\sigma}{2\rho_l r_0^2}(1-\xi^2)\xi^2 \tag{40}$$

where ξ is defined as the wave ratio ($\xi = \frac{2\pi}{\lambda} r_0$) and I_n, K_n are the nth order modified Bessel function of the first and second kind. In case of an inviscid liquid jet with no effect of the ambient gas, the above equation reduces to linear theory of Rayleigh [[61]]:

$$\omega^2 = \frac{\sigma}{\rho_l r_0^2}(1-\xi^2)\xi^2\frac{I_1(\xi)}{I_0(\xi)} \tag{41}$$

The numerical simulation of the capillary instability of an inviscid cylindrical liquid jet with neglecting gas effect in form of the growth rate is compared with the results of the linear theory [[61]] and the experimental measurements [[62]].

It is assumed that, a cylindrical liquid jet with undisturbed diameter D_0 =1.1mm is initially perturbed with a sinusoidal axisymmetric disturbance whose wavelength λ = 4.55D and its initial amplitude $\eta_0 = 0.00001D_0$. This small initial disturbance amplitude indicates that the dynamic instability of a liquid jet can be affected by relatively small perturbations induced by some mechanical device with a minimal energy input. The characteristic time scale of the performed case is $\tau = \left(\sigma/\rho_l r_0^3\right)^{0.5} = 648.7S^{-1}$, and the dimensionless growth rate is described as $\varpi = \omega/\tau$.

According to the linear theory, the variation of the logarithmic value of the amplitude is linear.

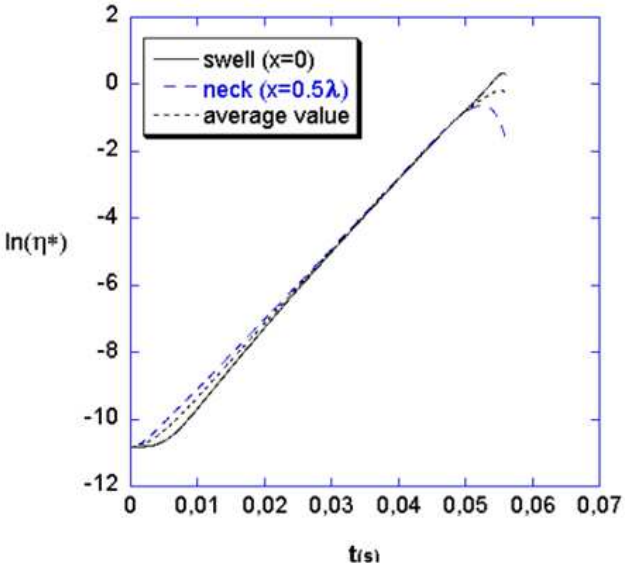

Figure 4. Logarithmic value of the dimensionless.

Figure 4 shows the calculated logarithmic value of the dimensionless amplitudes of the surface disturbance, ($\eta^* = \eta_0 / r_0$), for a wave ratio $\xi = 0.7$ that corresponding to the maximum growth rate obtained from the linear theory. The values are taken on the swell and neck of the wave. The average value of the both is plotted as well. The results show that in general the exponential growth rate of the surface disturbance is constant, as the linear behaviour of the logarithmic of the disturbance amplitude is reproduced.

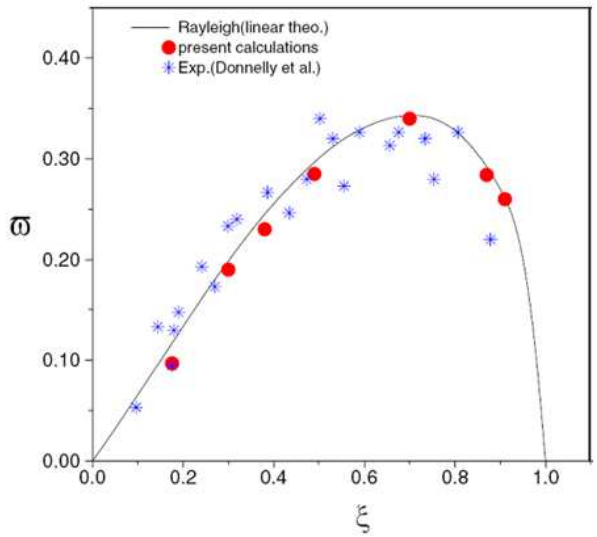

Figure 5. Comparison of the numericalamplitudes of the surface disturbance for results with the linear theory and the a wave ratio $\xi = 0.7$ experimental measurements.

Figure 5 presents the numerical results of the growth rate as a function of the wave ratio ξ . The results are compared with both the analytical solution obtained from the linear theory of Rayleigh [[61]],along with that the experimental measurements [[62]]. It can be seen that, in general, the

numerical results are in a good agreement with the linear theory for the wave ratios considered. A good agreement with the experimental results also has been obtained. The small discrepancies of the calculated results from the linear theory in the range of $0 \le \xi \le 0.7$ are due to the fact that the nonlinear effects are more effective for larger wavelengths, i.e. for small wave ratios.

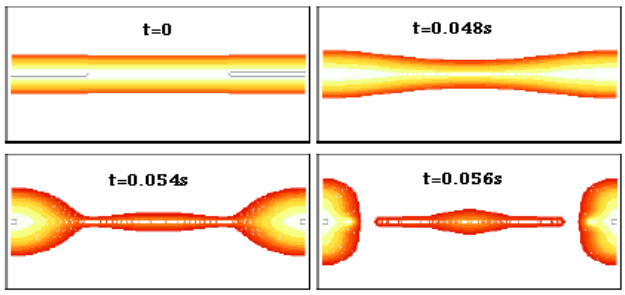

Figure 6. The topological change of a cylindrical liquid jet with initial disturbance ($\xi = 0.7$) at different time intervals.

Figure 6 shows the topological changes and break-up of a cylindrical liquid jet with initial disturbance whose wave ratio $\xi = 0.7$ corresponding to the maximum growth rate obtained from the linear theory [[61]].

The first surface shape is at initial time, where the small disturbance is imposed on the jet surface. The second shape at t = 0.048s corresponds to a point just after the jet enters into the nonlinear regime of its growth. At this time, the maximum and the minimum radii of the surface are the points that correspond to the initial peak and trough of the wave. They grow at the same rate, and their magnitude during the initial stages of the process can be computed by means of the linear theory. Therefore, the disturbance basically grows resembling the linear theory, and stays sinusoidal until this time. The next surface shape shown is at t = 0.054s, well into the nonlinear regime and just before the pinching process occurs. At this time, the surface tension driven motion is highly nonlinear, which leads to the formation of a thin ligament around the trough part of the wave. The ends of this fluid ligament are connected to the large mother drops originating from the crest parts of the wave. The further contraction of these ends leads to the pinching process that makes up the satellite drops. The formation of the satellite drops is considered to be a nonlinear phenomenon in the latter stages of jet breakup process. Finally, at time t = 0.056s the wave is divided into two mother drops and a thin ligament with a swelling in the centre. This swelling in the middle of the ligament reveals the reverse axial motion of the fluid after the breakup. Thereafter, the fluid ligament could be further deformed and may breakup.

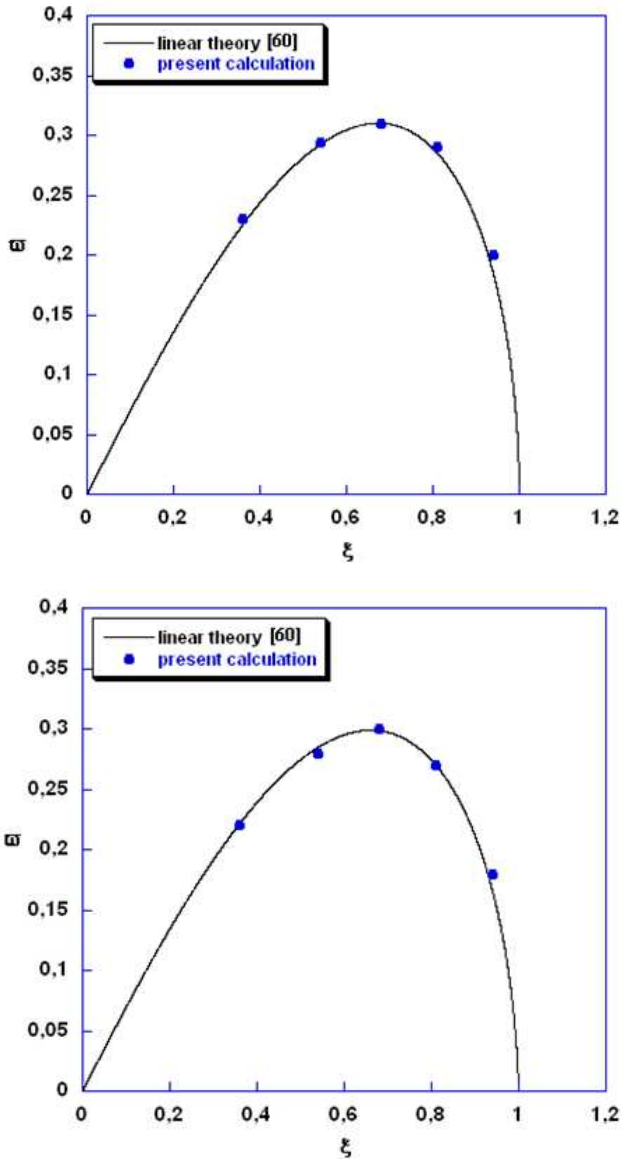

Figure 7. Comparison of the dimensionless growth rate with the linear theory for viscous liquid jet at different wave ratios.

Assuming that the viscous force is very great compared with the inertia force and neglecting the effect of the latter. Consequently, the evolution of the fluid filament is described by Stokes equation. For this case, the numerical simulation can be compared with Sterling and Sleicher theory [[60]]. The calculated growth rate is made dimensionless as in the simulation of Rayleigh instability. The simulations are performed for different wave ratios and by using two different values for the liquid kinematic viscosity, $\nu_l = 1\times10^{-6}\, m^2/s$ and $\nu_l = 5\times10^{-6}\, m^2/s$. Figure (7a, b) illustrates the comparison of the calculated dimensionless growth rate with that obtained from the linear theory [[60]]. The comparison indicates that, the numerical model predicts well the growth rate that calculated using the linear theory for both values of kinematic viscosity considered.

It is well known that, the viscosity can considerably alter the results of Rayleigh breakup for inviscid liquid jet. Therefore, a numerical simulation of a typical deformation and breakup of long viscous liquid threads is performed. An important feature for relatively low viscosity systems is that the breakup mechanism is self repeating in the sense that every pinch-off is always associated with the formation of a neck, the neck undergoes pinch-off, and the process repeats. In the later stages of the breakup, a slender tube around the trough part of the wave is formed. The pinching process of this ligament leads finally to the breakup forming satellite drops between the two mother drops. At the pinch point, the radius of the filament gets smaller, and the curvature goes to infinity, as a sequence, the time scale becomes shorter. Thus the velocity becomes very large, and the fluid left in the pinch region is driven by increasingly strong forces. This breakup process leads to the formation of satellite and sub-satellite droplets. Most of the numerical methods applied for two-phase flow simulation failed to predict this highly nonlinear phenomena and failed as well to continue through and after the pinching process. Therefore, in general, a detailed numerical analysis of the problem of satellite formation is difficult as a result of the associated numerical problems.

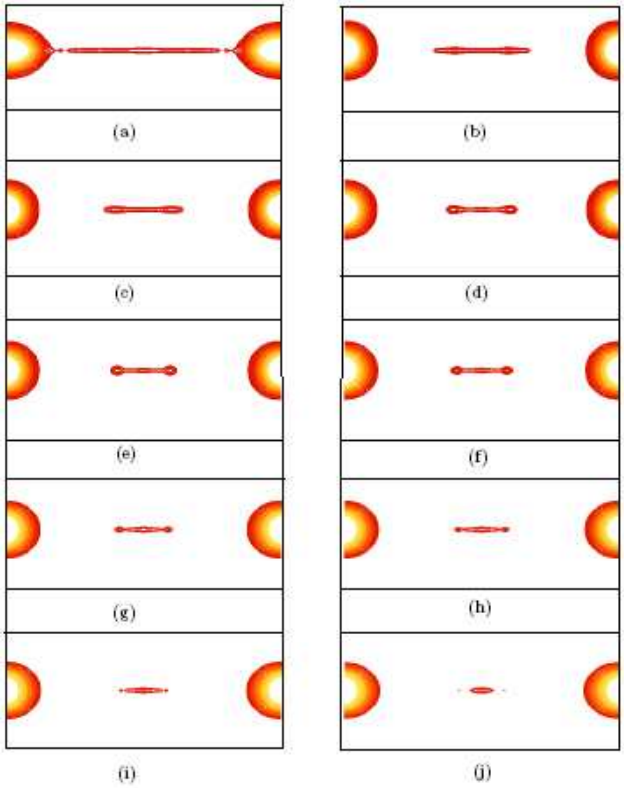

Figure 8. Collapse of satellite and subsatellite formation, for wave ratio of $\xi = 0.54$ and $Oh = \mu_l / \sqrt{\rho_l \sigma\, r_0} = 0.017$, 149 × 80 grid points, at t=0.1887, 0.1944, 0.1952, 0.196, 0.1968, 0.1976, 0.198, 0.1982, 0.1984, 0.199 s.

In order to focus on the satellite droplet formation and its multiple breakup process, a numerical simulation for wave ratio of $\xi = 0.54$ and with Ohnesorge number $Oh = \mu_l / \sqrt{\rho_l \sigma\, r_0} = 0.017$ is performed. The development and the collapse of the satellite droplets at later stages of the breakup process is illustrated in figure 8. The topological changes, shown in figure 8, consist of a relatively rapid bulbing of the end of the satellite drop followed by break-off of the bulbous ends from the central portion. This breakup process is known as"end pinching". The development of these bulbous ends is due to the internal driven motion of the filament. The observed self-repeating breakup mechanism is considered as important features of breakup of liquid jets with relatively low viscosity. Finally, there is a number of satellite and sub-satellite droplets exist between the two mother drops. At least three visible droplets are created in the central region. The predicted satellite droplets and the formation of sub-satellite droplets show the remarkable capability of the numerical procedure used. In general, the present numerical model predicts the capillary instability as well as the formation of satellite dropletss in the viscous regime, where the viscosity controls its subsequent breakup in a self repeating manner. This is considered as a great validation of the present developed numerical model as the calculations are capable to continue throughout the pinching process and droplet formation stage without any further numerical considerations.

4.2. Liquid Surface Deformation Due to Impinging Process

The impingement of an axisymmetric gaseous jet through lances upon a liquid surface or a molten bath is relevant in industrial and metallurgical processes, e.g. dust removal from the producer gas obtained from biomass gasification and electrical arc furnace steel production. As a result of the kinetic energy of the jet stream, the surface of the liquid will be depressed and a cavity is created on the surface of the liquid, as shown in figure 9. The experimental visualization of such cavity formation is a difficult task, so that the structure of the jet impingement on a liquid surface is not completely understood [[63]]. Consequently, a clear understanding of the impingement process is required through the numerical treatment.

The important characteristics in such process are the interface shape, cavity depth and width, lip formation and the recirculation pattern in the liquid. An extended review of the most important articles concerned such impinging process can be found in [[63]]. The problem configuration is shown in figure 9-a, while figure 9-b shows the analysis of forces acting upon the liquid surface during the impinging process.

The parameters described in the previous figure for the jetting system are given as follows; the nozzle diameter D_n,

vessel diameter D_c, the height of the undisturbed liquid H, distance between nozzle tip and liquid surface h, cavity depth h_c, cavity diameter d_c, lip height h_L, and the momentum of the jet is given by $M = 0.25\pi D_n^2 \rho_g V_j^2$, where ρ_g and V_j is the gas jet density and velocity, respectively. The Reynolds number, consequently, is given by $\mathrm{Re} = \rho_g V_j D_n / \mu_g$. On the other hand, the schematic of the force analysis can be seen in figure 9-b, where F_m, F_τ, F_p, F_σ, and F_g are the associated forces due to jet momentum, tangential shear stress, pressure force due to recirculatory flow, surface tension force and gravity force.

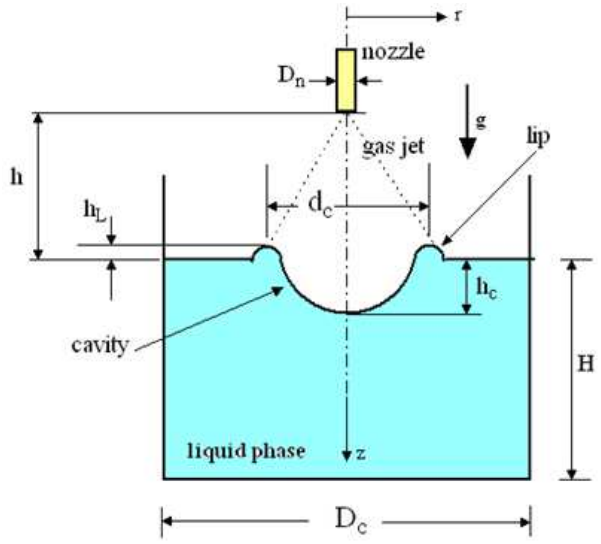

(a)

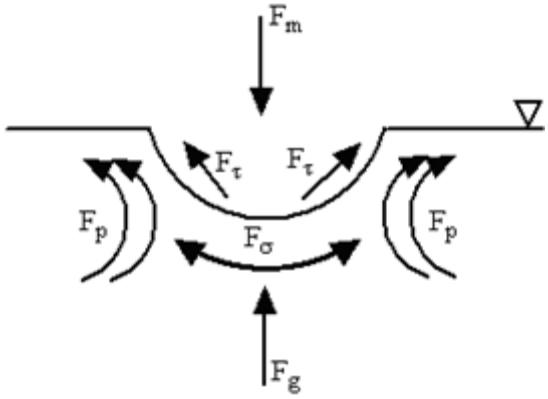

(b)

Figure 9. (a) the features of the jetting system and (b) the force analysis exerted upon the liquid surface.

In contrast to the continuous surface stress technique (CSS) [[28]] and the continuous surface force (CSF) technique [[35]], in the present algorithm, all these forces are modeled as interfacial forces which represent the pressure boundary conditions at the interfacial marker points on the interface. The loss of accuracy of CSF and CSS techniques can be seen in the numerical simulation of the deformation of a spherical drop under surface tension effects. In such cases, the kinetic energy does not decay to zero, (despite the physical and numerical dissipation), as a result of the so-called "*spurious currents*", which pose a challenge for the numerical simulation of bubble and droplet motion. In the present case, the statistically steady state cavity shape formed due to jet impingement should be obtained after a specified period of time corresponding to the operating parameters. This can only be achieved if the interfacial forces are dynamically balanced; i.e.

$$F_m + F_\tau + F_p + F_g + F_\sigma = 0 \tag{42}$$

The problem of how to numerically formulate these interfacial boundary conditions is, however, not completely solved. When the associated modeling of such interfacial forces is not accurate, consequently, it is expected that no statically steady state cavity will be obtained. Therefore, the obtained steady state cavity shape over large time intervals is considered as a challenge problem of such simulations and a challenge validation for our developed numerical method.

The characteristics of the cavity formed in the impinging process are dependent on the properties of the impinging jet as well as the liquid properties. When the jet momentum is small, a steady state cavity is just formed. On the other hand, a lip can appear at larger jet momentum. Further large jet momentum causes splash and ripples on the liquid surface. The present computation does not consider splash and ripples.

In order to combine the effect of the operating parameters as well as the fluids properties in such jetting system, the dimensional analysis theory is applied to obtain a new dimensionless number; we call here the Impinging number (*IM*), which can describe the impinging process in terms of the gaseous jet and the liquid bulk properties. The *IM* number is expressed as:

$$IM = \frac{\rho_g V_j D_n}{\mu_g} \cdot \frac{\sqrt{\rho_l \sigma H}}{\mu_l} \tag{43}$$

The above equation can be written in form of the known dimensionless number, Reynolds number (*Re*) and Ohnesorge number (*Oh*), as follows:

$$IM = \frac{\mathrm{Re}}{Oh} \tag{44}$$

The Reynolds number is considered as a measure of the jet momentum while the dimensionless Ohnesorge number measures the ratio of the viscous force on an element of fluid to the surface tension and the inertia force. The combination of both numbers could describe the strength of the impinging process adequately.

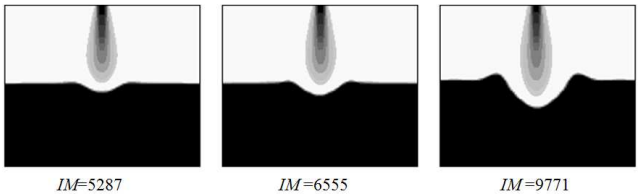

Figure 10. Effect of IM number on the formed cavity profiles and dimples formation at statistically steady state.

The preliminary results of the case under consideration, by using the *STD k-ε* model, have shown a little effect of the surface tension on the impinging process and a slightly reasonable effect of the liquid viscosity. Consequently, in the present numerical experiment, the Ohnesorge number is taken constant and equals 0.94, while the jet velocity is changed to obtain a wide range of *Re* number and consequently a wide range of *IM* number.

Figure 10 shows the effect of the *IM* number on the obtained statistically steady cavity profiles. Different *IM* numbers, ranging from small to medium and large numbers for jet spacing of (h= 5cm), are applied. The formation of dimples is clearly evident only at relatively high *IM* number. At low IM number, the dimples formed die out due to dissipation of their energy by viscous friction.

The circulation of the liquid and the velocity vectors in both phases are shown in figure 11-a, while the level set contours are illustrated in figure 11-b at *IM*=9771 and a jet distance of h=5cm. The tangential flow and the development of the recirculation regions are clearly visible with a center of the circulating flow in the liquid phase close to the centerline. It can also be seen that, in the opposite direction to the impinging jet, upward flows is built up due to the circulation initiated in the liquid phase. The existence of such upward flows, to some extent, can be considered as a stabilizing force that could prevent further increase of the cavity depth.

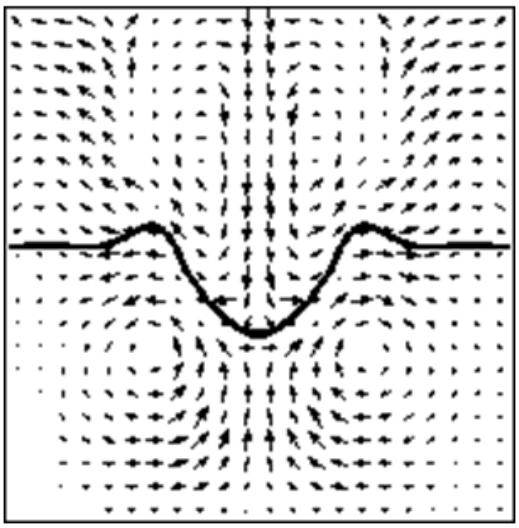

(a)

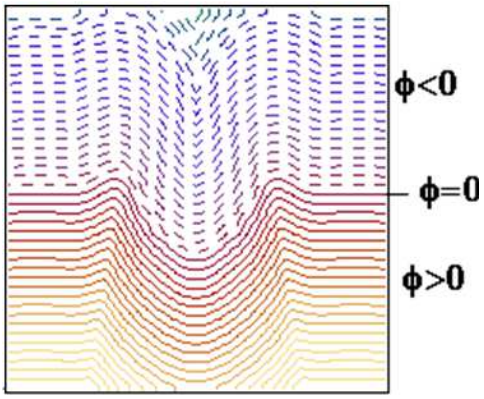

(b)

Figure 11. Velocity vectors (a) and level set contours (b) in both phases at IM=9771 and jet spacing h=5cm.

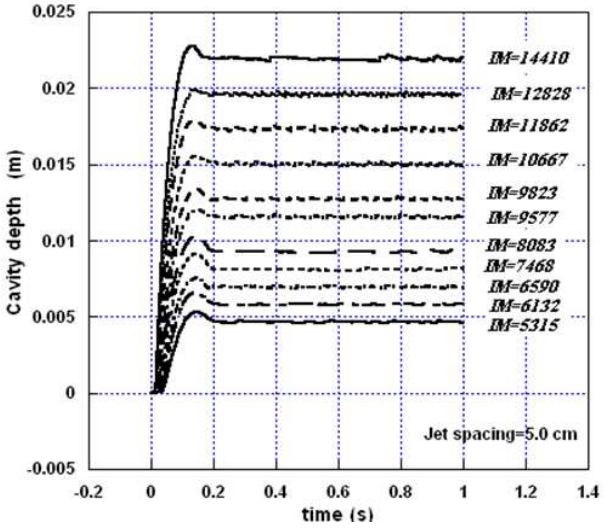

(a)

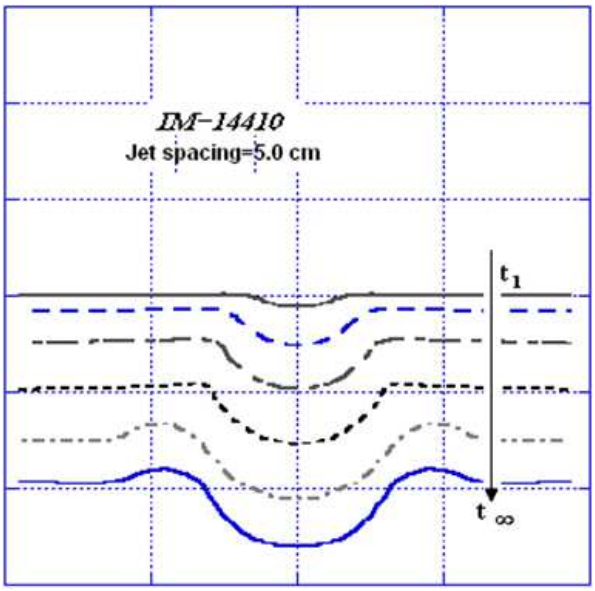

(b)

Figure 12. The time evolution of the cavity depth and shape during the jetting process; (a)for a wide range of *IM* numbers (b) at different time intervals.

The level set contours obtained in figure 11-b reveals the capability of the present developed level set technique in capturing the complex topological changes of the interface, especially the lip formation at the ends of the formed cavity.

An important feature of the present case, which also considered as a challenge problem, is the obtaining of the stead cavity profile over a large period of time. The statistically steady cavity profile obtained reveals the high accurate modeling implemented for the interfacial forces presented at the interface in the case considered.

Figure (12-a) shows the evolution of the cavity depth for a wide range of *IM* numbers during the jetting process until it reaches to an equilibrium position with observable small periodic oscillation of the cavity depth about this equilibrium position. In figure 12-b, the time evolutions of the topological changes of the liquid interface are illustrated. It can be seen that the liquid interface is stable within the first few seconds until the liquid jet start to impinge the liquid surface and then the cavity is formed. The pressure force of the impinging jet which is provided by the momentum flux of the gaseous jet causes the liquid surface to deform whereby a cavity is formed with a specified depth. Consequently, a lateral flow is developed and moved over the liquid surface generating a shearing force along the surface that drives the liquid towards the walls of the cylinder and producing symmetrically recirculation cells on both sides of the cavity, as shown previously (cf. figure 11-a). The equilibrium position is obtained when all the driving forces are dynamically balanced. In almost all cases, the cavity depth reaches a maximum value after a specified time as the liquid moves downward and then it rises again in a direction opposite to the gravity in order to satisfy the continuity by refilling the cavity created by the air jet impingement, then the cavity depth remains almost constant with an oscillation around an average value.

The most important parameters of the formed cavity are the interface shape, the width and the depth of the cavity and the height of the peripheral lip. Therefore, the numerical prediction of such parameters should be evaluated by comparing the obtained results with those predicted either analytically [[64]] or measured experimentally [[65]]. Consequently, a series of numerical experiments has bee performed with a wide range of the *IM* number by using both the STD turbulence model and the nonlinear turbulence model.

The comparison of the cavity depth and the cavity radius with the available analytical and experimental data is illustrated in figure 13 (a - b). The jet spacing is considered to be constant (h=5cm) for all numerical experiments. The comparison of the numerically predicted cavity depth shown in figure 13-a reveals that the numerical results obtained by using both turbulence models are in good agreement with the experimental measurements rather than the analytical prediction. This can be attributed to the fact that the theory did not take into account the effects of shear and surface tension forces as well as the existence of recirculation in the liquid phase. The return flow at higher *IM* number was therefore not expected to encounter any retardation.

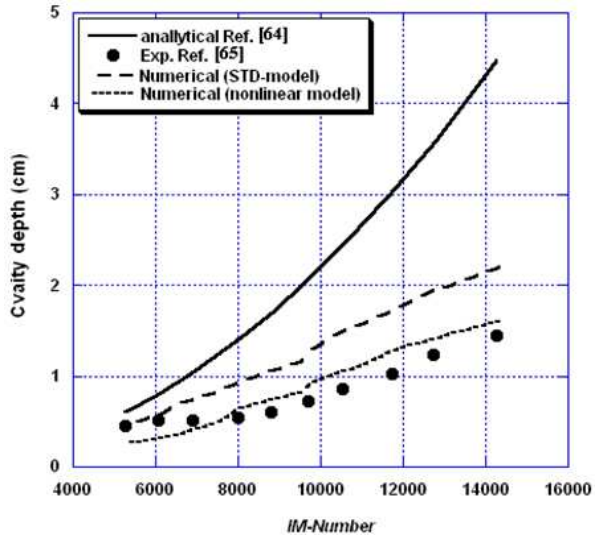

(a)

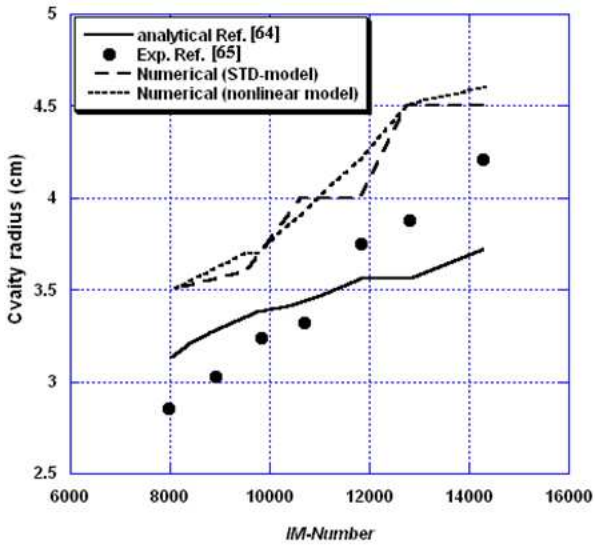

(b)

Figure 13. Comparison of the numerical results with the experimental and theoretical data for cavity depth (a) and cavity radius (b).

By comparing both turbulence models adopted, it can be seen that the numerical results obtained from the nonlinear turbulence model are in closer agreement with the experimental date than the results obtained from the STD model. The overestimated cavity depth, obtained from the STD model, can be referred to the excessive generation of the turbulent production at the impinging point with the

liquid surface. This is a general problem of linear turbulence models which produce incorrect prediction of anisotropic turbulence in many industrial important flows; e.g. impinging jets. Consequently, the accurate flow field prediction was not well predicted at the stagnation point where gas jet impinging the liquid surface, see for more details [[20]].

The comparison of the cavity radius, shown in figure 13-b, illustrates that the present numerical results from both linear and nonlinear turbulence models overpredict both of the experimental measurements and the analytical prediction.

However, the experimental trend is well numerically predicted. It should be pointed out that a part of the disagreement may be attributed to both of the associated error in the measurement of the cavity width due to liquid splashing and, from the other point, the crude assumption of the analytical predictions. At large *IM* number, the shear forces overcomes the surface tension force and, consequently, a separation is experimentally observed to occur at the cavity lips thereby producing "splashing" that can contribute to the error in measurements of the cavity radius [[65]]. On the other side, the lip formation phenomena could not be predicted analytically, and therefore, there is uncertainty in the theoretical definition of the cavity width. The present numerical prediction of the cavity radius indicates that no significant difference has been obtained by using either STD or nonlinear turbulence models. This implies that the tangential stresses predicted from both turbulence models are nearly equal. In general, the increase in the cavity depth and radius with the *IM* number is clearly evident.

The nonlinear turbulence model is now used for predicting the centerline velocity, V_{CL}, starting from the nozzle exit. The numerical results are compared with the analytical equation developed in [[66]] and based on the theoretical analysis provided by [[67]]:

$$\frac{V_{CL}}{V_J} = \frac{B}{z/D_n + B} \tag{45}$$

where B is a function of the gas jet Reynolds number and is given a value of 7.6 for the specified case listed below [[66]]:

Table 1. Parameters for the case study as specified in [66].

Dn(mm)	DC(mm)	h(mm)	H(mm)	VJ(m/s)
6	290	154	111	56.2

It should be pointed out that, the above equation, Eq. 45, has been used for validating the numerical results obtained from the commercial CFD code, Fluent, [[68]], however, for other cases and with different B-values.

Figure 14 shows the comparison between the centerline jet velocity, predicted by using the linear and the nonlinear turbulence models adopted, and the numerical results of Eq. 45. It can be seen that the predicted numerical results from both turbulence models agree well with the analytical solution provided by Eq.45 nearly up to the point at which the jet enters the cavity region (at $z/D_n \approx 60$). The not observed differences between the linear and the nonlinear turbulence models adopted in predicting the man centerline velocity reveals that the nonlinear constitutive relation has no effect over the prediction of the mean variables. However, the nonlinear formulation has a significant effect on the cavity depth which influenced by the correct prediction of the anisotropic stresses at the impinging region (cf. figure 13-a). Consequently, detailed analysis of the Reynolds stresses should be investigated further in our future work.

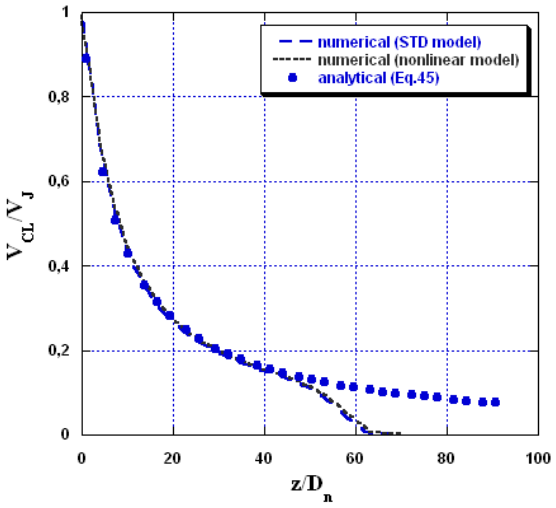

Figure 14. Comparison of the predicted centerline jet velocity with the analytical solution [[66]].

5. Conclusion

A new interfacial marker-level set method (IMLS, which could provide an accurate and robust prediction of the two-phase flow dynamics with moving interface, has been developed. The governing unsteady RANS-equations are coupled with the level set method and solved in each phase separately on structured cell-centered collocated grids using the control volume approach on the physical domain of the problem considered. A consistent balance of kinematic and dynamic interfacial conditions on the interface has been described by a general equation that collects all the expected interfacial stresses. By fitting a number of interfacial markers on the intersection points of computational grids with the interface, the interfacial stresses and consequently the interfacial driving forces are easily estimated. Moreover, the normal interface velocity, calculated at the interfacial markers position, can be extended to the higher dimensional level set function and applied for the advection algorithm of the level set method. The present method has been applied

for a wide range of numerical experiments either in laminar or turbulent complex two-phase flows. The capillary instability of a cylindrical liquid jet in linear and nonlinear regimes has been numerically simulated and the results are evaluated through the comparison with the linear theory and the available experimental measurements. The effect of viscosity on the breakup mechanism of the cylindrical liquid jet and the satellite/subsatellite formation has been investigated.

The developed numerical method has been further extended to simulate one of the most challenge problem in two-phase flows; namely, the impinging of turbulent gaseous jet onto a liquid surface. Both linear and nonlinear turbulence models have been applied to predict the turbulent flow characteristics and surface deformation. According to our background, this is the first time to implement the nonlinear turbulence model in the numerical simulation of turbulent two-phase flows with moving interfaces. The numerical results obtained show high performance of the nonlinear turbulence model over the STD k-ε model in predicting the parameters associated with the anisotropic stresses. However, a similar prediction from both turbulence models has been obtained fro the mean variables or the tangential stresses.

In general, the developed IMLS method demonstrates a remarkable capability to predict the dynamical characteristics of either laminar or turbulent complex two-phase flow in many industrial and engineering applications.

References

[1] Lefebvre, A. H., Atomization and sprays, Hemisphere Publishing Corporation, 1989.

[2] Won, H. and Peters, N., Investigation of cluster-nozzle concepts for direct injection diesel engines, Atomization and sprays, Vol. 19(10), pp. 983-996, 2009.

[3] Garbero, M., Vanni, M. and Fritsching, U., Gas/Surface heat transfer in spray deposition processes, Int. J. Heat and Fluid Flow, Vol.(27), pp. 105-122, 2006.

[4] Torpey PA., Prevention of air ingestion in a thermal ink-jet device. Proceedings of the 4th International Congress on Advances in Non-impact Print Technologies, Springfield, VA, March 1988.

[5] Dressler, D., Li, L., Green, S., Davy, M. and Eadie, D., Newtonian and non-newtonian spray interaction with a high-speed moving surface, Atomization and sprays, Vol. 19(1), pp. 19-39, 2009

[6] Zhaorui Li, Farhad A. Jaberi1 and Tom I-P. Shih, A hybrid Lagrangian–Eulerian particle-level set method for numerical simulations of two-fluid turbulent flows, Int. J. Num. Methods in Fluids, Vol 56, pp. 2271-2300, 2008.

[7] Desjardins, O., Moureau, V. and Pitsch, H., An accurate conservative level set/ghost fluid method for simulationg turbulent atomization, J. Comp. Physics, Vol. 227, pp. 8395-8416, 2008.

[8] Herrmann, M., A Eulerian level set/vortex sheet method for two-phase interface dynamics, J. Comp: Physics, Vol. 203, pp. 539-571, 2005.

[9] Eggers, J., Nonlinear dynamics and breakup of free-surface flows, Reviews of modern physics, Vol. 69(3), pp. 1-65, 1997.

[10] Schulkes, R. M., The evolution and bifurcation of a pendant drop, J. Fluid Mechanics, Vol. 278, pp. 83-100, 1994.

[11] Borue V, Orszag SA, Staroselsky I., Interaction of surface waves with turbulence: direct numerical simulations of turbulent open-channel flow. Journal of Fluid Mechanics, Vol. 286, pp. 1–23, 1995.

[12] Pan Y, Banerjee S., A numerical study of free surface turbulence in channel flow, The Physics of Fluids; Vol. 7, pp. 1649 –1664, 1995.

[13] Tsai W-T., A numerical study of the evolution and structure of a turbulent shear layer under a free surface, Journal of Fluid Mechanics, Vol. 354, pp. 239 –276, 1998.

[14] Scardovelli R, Zaleski S., Direct numerical simulation of free-surface and interfacial flow, Annual Review of Fluid Mechanics, Vol. 31, pp. 567–603, 1999.

[15] Rhea, S., Bini, M., Fairweather, M. and Jones, W.P., RANS modelling and LES of a single-phase, impinging plan jet, Computers and Chemical Engineering, Vol. 33, pp. 1344–1353, 2009.

[16] Launder BE, Spalding DB. The numerical computation of turbulent flows. International Journal for Numerical Methods in Fluids, Vol. 15, pp. 127–146, 1974.

[17] Rodi W. Turbulence models and their applications in hydraulics. International Association of Hydraulic Research, Delft, the Netherlands, Monografy, 1980.

[18] El-Askary, W. and Balabel, A., Prediction of reattachment turbulent shear flow in asymmetric divergent channel using linear and non-linear turbulence models, Eng. Research Journa (ERJ), Faculty of Eng., Menoufiya Uni., Vol.30(4), pp. 535-550, 2007.

[19] Pope, S. B., A more general effective-viscosity hypothesis, J. Fluid Mech., 72, 331-340, 1975.

[20] Craft, T. J., Launder, B. E., and Suga, K., Development and Application of a Cubic Eddy-Viscosity Model of Turbulence, International Journal of Heat and Fluid flow, Vol. 17, pp.108-115, 1996.

[21] Apsley, D. D. and Leschziner, M. A., A new low Re non-linear two-equation turbulence model for complex flows, Proc. 11th Symposium on Turbulent Shear Flows, Grenoble, 1997.

[22] Popinet S, Zaleski S, Afront tracking algorithm for the accurate representation of surface tension, Int. J. Numer. Meth. Fluids, Vol. 30, pp. 775–793, 1999.

[23] Unverdi SO, Tryggvason G., A front-tracking method for viscous, incompressible, multi-fluid flows, Journal of Computational Physics, Vol. 100, pp. 25–37, 1992.

[24] Nichols B D, Hirt C W, Methods for calculating multi-dimensional, transient free surface flows past bodies, Proc. First Int. Conf. Num. Ship Hydrodynamics Gaithersburg, pp. 20–23, 1975.

[25] Osher S, Sethian JA., Fronts propagating with curvature-dependent speed: algorithms based on Hamilton–Jacobi formulations, Journal of Computational Physics, Vol. 79, pp. 12–49, 1988.

[26] Peters, N., Turbulent combustion, Cambridge University Press, Cambridge, UK, 2000.

[27] Pierre T., Stephane, V., Jean-Luc E. and Jean-Paul C., Detailed comparisons of front-capturing methods for turbulent two-phase flow simulations, Int. J. Num. Meth. Fluids, Vol. 56, pp. 1543-1549, 2008.

[28] Lafaurie, B., Nardone, C., Scardovelli, R., Zaleski, S. and Zanetti, G., Modelling, merging and fragmentation in multiphase flows with SURFER, J. Comp. Physics, Vol. 113, pp. 134-147, 1994.

[29] Albert, Y. T. and Zhaoyuan, W., A numerical method for capillary-dominant free surface flows, J. Comp. Physics, Vol. 221, pp. 506-523, 2007.

[30] Enright, D., Fedkiw, R. , Ferziger, J. and Mitchell, I., A hybrid particle level set method for improved interface capturing, J. Comp. Physics, Vol. 183, pp. 83-116, 2002.

[31] Herrmann, M., A Eulerian level set/vortex sheet method for two-phase interface dynamics, J. Comp. Physics, Vol. 203, pp. 539-571, 2005.

[32] Garzon, M., Gray, L. J. and Sethian, J. A., Numerical simulation of non-viscous liquid pinch-off using a coupled level set-boundary integral method, J. Comp. Physics, Vol. 228, pp. 6079-6106, 2009.

[33] Sussman, M. , Smereka, P. and Osher, S., A level set approach for computing solutions to incompressible two-phase flows, J. Comp. Physics, Vol. 114, pp. 146-159, 1994.

[34] Sethian, J. A. and Smereka, P., Level Set Methods for Fluid Interfaces, Annu. Rev. Fluid. Mech., Vol. 35, pp. 341-372, 2003.

[35] Brackbill, J. U., Kothe, D. B. and Zemach. A, , A Continuum Method for Modeling Surface Tension, J. Comp.Phys., vol. 100, pp. 335-354, 1992.

[36] Ierley, G. and Shkoller, S., Smoothing the wrinkles: a new model for surface tension, J. Fluid Mech., Preprint (2002).

[37] Balabel, A., Numerical simulation of Gas-Liquid interface dynamics using the level set method, Dissertation, RWTH Aachen, Germany, 2002.

[38] Balabel, A., Binninger, B., Herrmann, M. and Peters, N., Calculation of Droplet Deformation by Surface Tension Effects using the Level Set Method, J. Combustion Science and Technology, Vol. 174 (11,12), pp. 257-278, 2002.

[39] Balabel, A., Numerical investigation of the binary droplet collision in incompressible continuum fluids using the level set method, submitted for publication in Computers and Fluids, 2010.

[40] Craft, T.J., Launder, B.E. and Suga, K., Development and application of a cubic eddy-viscosity model of turbulence. International Journal of Heat and Fluid Flow, Vol.17, pp. 108-115, 1996.

[41] Craft, T.J., Iacovides, H. and Mostafa, N. A., Modelling of three-dimensional jet array impingement and heat transfer on a concave surface. International Journal of Heat and Fluid Flow, Vol.29, pp. 687-702, 2008.

[42] Craft, T.J., Iacovides, H., Yoon, J.H., Progress in the use of non-linear two equation models in the computation of convective heat-transfer in impinging and separated flows, Turbul. Combust. Vol. 63, pp. 59–80, 1999.

[43] Launder BE, Spalding DB, The Numerical Computation of Turbulent Flows, International Journal for Numerical Methods in Fluids, 15:127-146, 1974.

[44] Osher, S. J. and Sethian, J. A., Front Propagation with curvature dependent speed: Algorithms based on Hamilton-Jacobi Formulation, J. Comp. Phys., Vol. 79, pp. 12-49, 1988.

[45] Sethian, J. A. and Smereka, P., Level set methods for fluid interfaces, Annu. Rev. Fluid, Mech., Vol. 35, pp. 341-372, 2003.

[46] Adalsteinsson, D. and Sethian, J. A., The fast construction of extension velocities in level set methods, J. Comp. Phys., Vol. 148, pp. 2-22, 1999.

[47] Sethian, J. A., A marching level set method for monotonically advancing fronts, Proceedings of the National Academy of Science, Vol. 93(4), pp. 1591-1595, 1996.

[48] Marangoni, C., Ueber die Ausbreitung der Tropfen einer Flüssigkeit auf der Oberfläche einer Anderen, Ann. Phys. Chem.; Vol. 143, pp. 337-354, 1871.

[49] Chang, Y. C., Hou, T. Y, Merriman, B. and Osher, S., A level set formulation of Eulerian interface capturing method for incompressible fluid flows, J. Comp. Phys., Vol. 124, pp. 449-464, 1996.

[50] Popinet, S. and Zaleski, S., A front-tracking algorithm for accurate representation of surface tension, Int. J. Numer. Meth. Fluids, Vol. 30, pp. 775-793, 1999.

[51] Zhongguo, S., Guang, Xi and Chen, Xi, Numerical simulation of binary collisions using a modified surface tension model with particle method, Nuclear Engineering and Design, Vol. 239, pp. 619-627, 2009.

[52] Landau, L. D. and Lifshitz, E. M., Fluid Mechanics, Pergamon London, 1959.

[53] Benjamin, T. B., Shearing Flow over a Wavy Boundary, J. Fluid Mech., vol. 6, pp. 161-205, 1959.

[54] Sterling, A. M. and Sleicher, C. A., The Instability of Capillary Jets, J. Fluid Mech., vol. 68 (3), pp. 477-495, 1975.

[55] Asali, J. C. and Hanratty, T. J., Ripples Generated on a Liquid Film at high Gas Velocities, J. Multiphase flow, vol. 19 (2), pp. 229-243, 1993.

[56] Watanabe, T., Numerical simulation of oscillations and rotations of a free liquid droplet using the level set method, Computers & Fluids, Vol. 37, pp. 91-98, 2008.

[57] Ierley, G. and Shkoller, S., Smoothing the wrinkles: a new model for surface tension, J. Fluid Mech., Preprint (2002).

[58] Fedkiw, R. P., Aslam, T., Merriman, B. and Osher, S. J., A non-Oscillatory Eulerian Approach to Interfaces in Multimaterial Flows (the Ghost Fluid Method), J. Comput. Phys., Vol. 154, pp. 393-427, 1999.

[59] Patankar, S. V., Numerical Heat Transfer and Fluid Flow, Hemisphere Publishing Corporation, 1980.

[60] Sterling. A. M. and Sleicher, C. A., The Instability of Capillary Jets, J. Fluid. Mechanics, Vol.68, pp. 477-495 , 1975.

[61] Rayleigh, L., On The Instability of Jets, Proc. Roy. Soc. London. Math. Soc., Vol. 10, pp. 4-13, 1878.

[62] Donnelly, R. J. and Glaberson, W., Experiments on the capillary instability of a liquid jet, Proc. Roy. Soc. A283, Vol.290, pp. 547-566, 1966.

[63] Nakazono, D., Abe, K., Nishida, M. and Kurita, k., Supersonic O2-jet impingement on liquid iron with surface chemistry, ISIJ International, Vol. 44 (1), pp. 91-99, 2004.

[64] Cheslak, F. R., Nicholls, J. A. and Sichel, M., Cavity formed on liquid surfaces by impinging gaseous jets, Journal of Fluid Mechanics, 36, pp. 55-64, 1969.

[65] Eletribi, S., Mukherjee, D. K. and Prasad, V., Experiments on Liquid Surface Deformation upon Impingement by a Gas Jet, Proceeding of the ASME Fluids Engineering Division, Vol. 244, pp. 235-247, 1997.

[66] Wakelin, D. E., The interaction between gas jest and the surface of liquids including molten metals, PhD, University of London, UK, 1996.

[67] Banks, R. B. and Chandrasekhara, D. V., Experimental investigation of the penetration of a high-velocity gas jet through a liquid surface, J. Fluid Mech., Vol. 15, pp. 13–34, 1963.

[68] Nguyen, Anh. V. and Evans, G. M., Computational fluid dynamics modelling of gas jets impinging onto liquid pools, Applied Mathematical Modelling, Vol. 30, pp. 1472–1484, 2006.